H.G. Esser, V. Philipps, P. Wienhold, K. Sugiyama, A. Kreter,
P. Coad, T. Tanabe and JET EFDA contributors

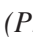# Post Mortem Analysis of a JET Quartz Microbalance System

Post Mortem Analysis of a JET Quartz Microbalance System

H.G. Esser[1], V. Philipps[1], P. Wienhold[1], K. Sugiyama[3], A. Kreter[1],
P. Coad[2], T. Tanabe[3] and JET EFDA contributors*

[1]*Institut für Plasmaphysik, Forschungszentrum Jülich GmbH, EURATOM Association,
Trilateral Euregio Cluster, D-52425 Jülich, Germany*
[2]*EURATOM/UKAEA Fusion Association, Culham Science Centre, Abingdon, OX14 3DB, UK*
[4]*Department of Nuclear Engineering, Graduate School of Engineering, Nagoya University,
Furo-cho, Chikusa-ku, Nagoya 464-8603, Japan*
* See annex of J. Pamela et al, "Overview of JET Results",
(Proc. 20th IAEA Fusion Energy Conference, Vilamoura, Portugal (2004).

ABSTRACT.

In the year 2001 a Quartz Microbalance System (QMB) was installed in the remote area of the inner JET divertor to measure in-situ erosion and redeposition processes. When removed in 2004, the system was found to be coated all over with carbon deposits. The deposit on the "deposition-quartz" and the outer and inner housing was characterized by various analysis methods to obtain additional information on the layer properties and to compare with the results obtained in situ during the exposure. The layer thickness was determined to 1.85 ± 0.1 mm in the average on an area of 0.95 cm^2 which must be related to the measured frequency change of 23640Hz , equivalent to 1.7×10^{-4}g. This corresponds to a carbon mass thickness of 9.3×10^{18} C atoms/cm^2. A significant deposition was also found on the surfaces inside the QMB housing which can only be explained assuming a high fraction of low sticking particles.

1. INTRODUCTION AND MOTIVATION

Understanding and modelling of wall erosion, material re-deposition and fuel (tritium) retention in fusion devices are vital for the development of fusion energy [1]. To improve our knowledge and database for modelling, a Quartz Microbalance System (QMB) was installed in JET in 2001[2]. It measured on-line and shot by shot layer deposition and possible re-erosion in the remote area of the inner divertor. Results of measurements carried out during 2001-2003 (campaigns C5 – C12) were presented in[3]. Local geometry (strike point position) was identified as a key parameter for deposition or possible erosion. Deposition increases significantly as the strike point approaches the louver entrance. Particles eroded previously were temporary stored on base tile 4 and subsequently transported into the remote area when the strike point was moved down to that tile. These shots showed highest deposition on the quartz with deposition rates of more then 10nm per shot. In the overall, high power Elmy-H-mode discharges with the strike point on tile 4 dominated the carbon deposition. These QMB results have been modelled by the ERO code confirming that the particle sources must be close to the QMB detector on tile 4 in order to produce a noticeable material deposition there[4]. After the end of the campaign the QMB system was removed remotely and colourful C- layers appeared on the quartz and on outer and inner surfaces, see figure 1. Those layers were characterized to complement the QMB in situ results and to improve our understanding of the local particle transport towards and inside the QMB housing.

2. EXPERIMENTAL

2.1. QMB HISTORY

The QMB system was operational from campaign 2001 to 2003 (C5-C12) for about 4000 shots and failed in 2003 due to overheating. The exposure time was 6479 seconds in total. The deposit caused a frequency shift of 23640 Hz corresponding to 1.77×10^{-4} g. However, layers had been formed all over the system varying from thin layers of a few nanometer on the sides not directly exposed to thicknesses much larger than 10 ºm on outer areas not protected by the QMB shutter. The layers on

the quartz itself and on internal surfaces behind the orifice of the outer heat shield were formed only when the QMB shutter was opened while the layer formation on the outer surfaces is continuously ongoing during the overall divertor plasma time, about 26.4hours. Thus, on the front side of the outer heat shield 4 different areas of deposition appeared, depending on shutter position, see figure 1. The layer next to the orifice was formed synchronously with the deposition on the quartz. The area hidden by the shutter is exposed when the shutter is closed, 24.6hours. The triangle left above the orifice is always exposed and another triangle of the same size behind the shutter is always hidden and has no layer. The thicknesses of those layers and thus erosion and deposition depend not only on the exposure time but also on local geometrical shielding effects and surface orientation.

2.2. GLOBAL AND LOCAL QMB GEOMETRY

Figure 2 illustrates the location of the QMB in the MKII GB SRP divertor. The QMB is fixed to a carrier rib of module 13, octant 5 shielded against power flux by tile 3. Only a small part of the QMB system with the orifice for the crystal is exposed to particle flux into the gap between horizontal tile 4 and vertical tile 3 which has a height of 29mm. The centre of the quartz is 16.25mm below the lower edge of tile 3 but protected by the shutter except for dedicated exposures.

2.3. GEOMETRY OF QMB HOUSING

Figure 3 shows a horizontal cut through the QMB housing across the quartz (1) which is a circular disc, 0.29mm thick and 14mm wide. Two 1mm thick stainless steel heat shields, one inner (3) and one outer(4) prevent electronic components on the circuit board (2) inside the copper box (5) from damage due to overheating. The distance between inner and outer heat shield is 5.5mm and between inner heat shield an the lid of the copper box 2mm. Circular orifices with diameters of 11 mm for the outer heat shield, 8mm for the inner heat shield and 14mm for the copper lid, define the particle flux channel to the quartz. The Quartz itself is attached from inside to the 1mm thick AL^2O^3 circuit board with a 11mm hole which limits the exposed quartz area to 0.95cm^2. All orifices are axially aligned with respect to the centre of the quartz. In total, the quartz is recessed by 13.5mm with respect to the outer heat shield. Fore more details see [2].

3. RESULTS

3.1. DEPOSIT ON THE DEPOSITION QUARTZ CRYSTAL

Figure 4 shows the quartz after exposure attached to the lid of the box. The line indicates its horizontal orientation in the divertor. The interference colours of the layer indicate inhomogeneous coating. Composition and thickness were analysed at the marks along the line across the quartz. SIMS (secondary ion mass spectroscopy) depth profiling has been done at marks 2, 3 and 4 in figure 4 confirming carbon hydrogen species and oxygen as the major elements. The depth profiles showed homogeneous distribution in depth down to the gold interface on the quartz. The thickness of the

layer was determined by means of step height measurements with a mechanical stylus profilometer. The thicknesses measured at the SIMS craters and the edges of the layer at the marks 1 and 5 are plotted in figure 5. They show a maximum thickness of 2.7μm near the centre dropping down to 1.6μm 1.0μm at the edges. The curve suggests a slight toroidal shift of the maximum of the thickness to the left side of the plot which is also supported by the colour pattern. This is the particle flux direction into the inner divertor. The thickness was confirmed by means of SEM (secondary electron microscopy) at a cross sectional fracture of the layer showing a thickness of 2.13μm at the mark R. This value is in excellent agreement with the stylus measurement as shown in figure 5. Based on these data an averaged thickness of 1.85 ± 0.15mm was deduced leading to a layer volume of 1.7×10^{-4} cm^3 and, using the mass increase measured by the frequency shift, a density of 0.95±0.1g/cm^3. TDS (thermal desorption spectroscopy) was used to determine the deuterium content in the layer. Two sections of the quartz were degassed by slow ramp heating up to 1000°C. 1.8 10^{18} D/cm^2 was found for sample 1 (20.7 mm^2) and 3.87×10^{18} D/cm^2 for sample 2 (14.6 mm^2). The fraction of hydrocarbon molecules to hydrogen released from the samples 1, 2 was 17 and 11% respectively with a minor contribution of C_2H_x indicating a more hard a-C:H layer. These values result in a D/C ratio of 0.19 for sample 1 respectively 0.41 for sample 2. The SIMS spectra showed clearly the appearance of tritium in the layer showing a symmetric depth profile with its maximum at about half of the layer thickness. The tritium originates from the trace tritium experiment (DTE1) performed during the campaign. The amount of T was quantified by means of calibrated IP (imaging plate[x]) measurements showing an average value of 1.95×10^{16} T-atoms/cm^2. Figure 6 shows a line scan across the quartz with a hollowed profile of the areal tritium concentration.

3.2 LAYERS ON THE INNER HEAT SHIELD

The diameter of the orifice of the inner heat shield is 3mm smaller than the outer one see, figure 3. Thus the impinging particles hit this protruding circular rim forming a nearly circular layer, see figure 7. However the carbon layer extends radially very deeply inside the slit up to a distance of about 25mm despite a distance of only 5.5mm between inner and outer heat shield. Again the deposition pattern maximum is shifted toridally similar as described for the quartz. The layer thickness was analysed by means of colorimetry [x] and the integral amount of C was deduced to 4.7×10^{18} C-atoms. The line scan across the orifice is seen in the red line figure 7. It reveals the highest layer thicknesses at the rim edges, 1.7μm respectively 1.3mm, showing the asymmetry described above. The tritium amount in that layer was determined by IP to 1.01×10^{16} T-atoms/cm^2. Interestingly, a circular layer was formed around the orifice also on the back side of the heat shield. Its maximum thickness is 0.7μm extending radially 10mm as shown in the curve II, figure 8. The total C-amount in this layer was determined to 1.46×10^{18} C-atoms.

3.3 DEPOSITS ON THE OUTER HEAT SHIELD

NRA (Nuclear Reaction Analysis) and RBS Rutherford back scattering) were done on the outer

heat shield since its tritium amount exceeded the exemption limit and hampered further analysis. The depth resolution of this method is given by the penetration depth of the incoming ion beam and about 8-10µm . An the outer area which was exposed all the operation time (26.4h) the layer thickness is well above this limit with high ratio of D/C.

3.4 DISCUSSION OF RESULTS

The in-situ measured mass increase of the deposit of $\sim1.8\times10^{-4}$ g deduced from the frequency shift and the averaged layer thickness on the quartz of 1.85µm determined here result in a layer density of ~0.95g/cm^3. This is comparable low for a-C:H layers but in line with results from deposition monitors used in JET[6]. The pattern of the layer thickness with a maximum near the centre indicates that the predominant particle flux direction is radial inward as can be seen e.g. form the fact that the orifice of the inner heat shield (8mm) is projected onto the quartz (11mm). The toroidal shift of the pattern, however, suggests a slight preferential toroidal particle direction in the direction of the particle flux into the divertor. This originates most probably from the preferential distribution of sputtered particles from tile 4 which should have this direction. The continues thickness transition from in the centre 2.7µm to about 1mm is due to local geometry effects with the centre of the quartz having in the average a larger solid angle to the particle sources then the edges. A significant contribution of low sticking species is required to explain the layer on the inner heat shield with an extension of about 25mm into a slit with a width of 5.5mm. Reflected and low sticking species form also the layer on the backside of the heat shield which has a maximum thickness of about half of that on the outer ring. The strong change of the T/C ratio across the quartz is explained by the influence of the substrate temperature on hydrogen co-deposition. The areal tritium concentration increases radial from the centre towards the edge of the layer by about a factor of 2 and the ratio T/C by a factor of 4 due to the reverse behaviour of the carbon profile. We believe that the power picked up during exposure causes a non uniform heating of the quartz due to the low thermal conductivity of 2W/mK und the low thickness of 0.29 mm and thus heat capacity of the quartz. This explains well the hollowed T profile as the differing values of the deuterium content obtained from the two TDS samples.

SUMMARY

A hydrogen rich carbon film with no detectable impurities (except oxygen) has been found on the QMB crystal with an averaged layer thickness of 1.85µm consistent with a density of ~ 0.95 g/cm^3 using the in situ measured mass increase of $\sim1.8\times10^{-4}$g. The deposition pattern shows a predominantly radial directed flux with some toroidal shift in the direction of the incoming particle flux to the inner divertor. A strong change of the T/C and D/C ratio across the quartz is observed which indicates hydrogen release during the deposition process by heating of the crystal due to the plasma power impact. A significant contribution of low sticking and reflected species must be assumed to explain the extension of the deposited layer into the slits of the housing and the backside of the heat shield.

4

REFERENCES:

[1]. G. Federici, C. H.Skinner, J.N. Brooks et al Nucl. Fusion, **41** (2001) 1967

[2]. H. G. Esser et al., Fusion Engineering and Design, **66-68** (2003) 855

[3]. H.G. Esser et al. J. Nucl. Materials **337-339** (2005) 84

[4]. A Kirschner at al. J. Nucl. Mat. **337-339** (2005) 17

[5]. Journal of Nuclear Materials, Volumes **313-316**, March 2003, Pages 507-513

[6]. Private communication Matej Mayer

[7]. P. Wienhold al., J. Nucl et. Mat. **176-177** (1990) 150 P.

Figure 1: QMB system before and after exposure.
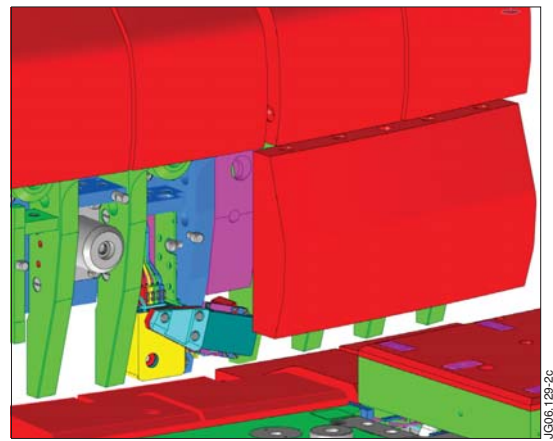
Figure 2: 3 dimensional view on QMB in remote area of inner divertor.
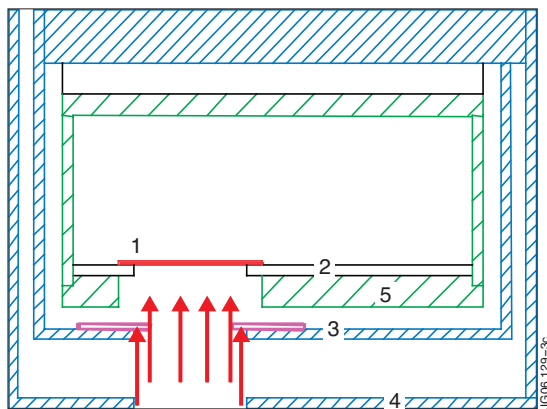
Figure 3: Cut of QMB-housing across the deposition-quartz
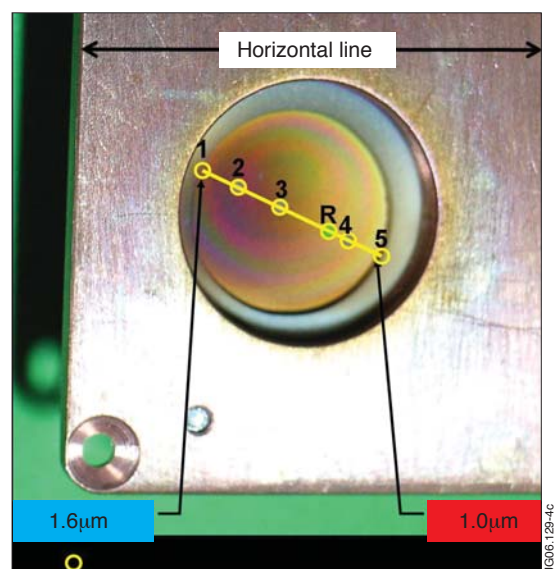
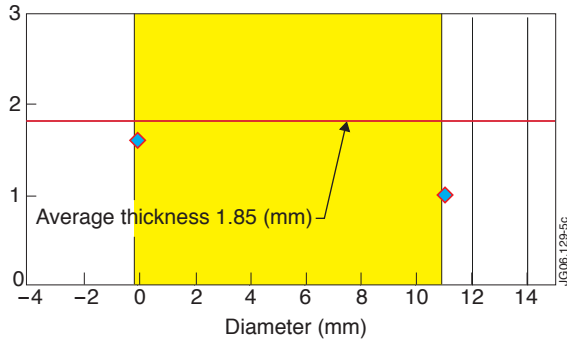*Figure 4: Amorphous hydrogen rich layer on deposition-quartz*

5

Figure 5: Determination of layer thickness on deposition-quartz
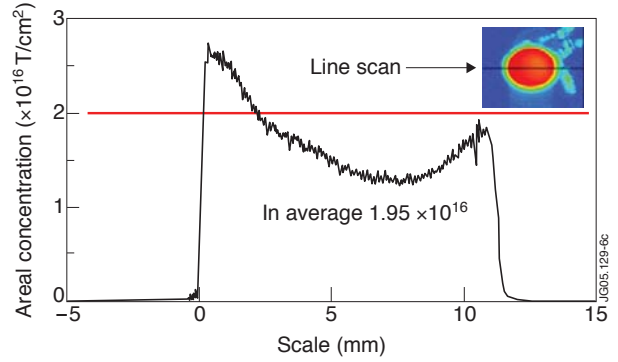

Figure 6: Calibrated line scan of tritium mass thickness across the deposition-quartz
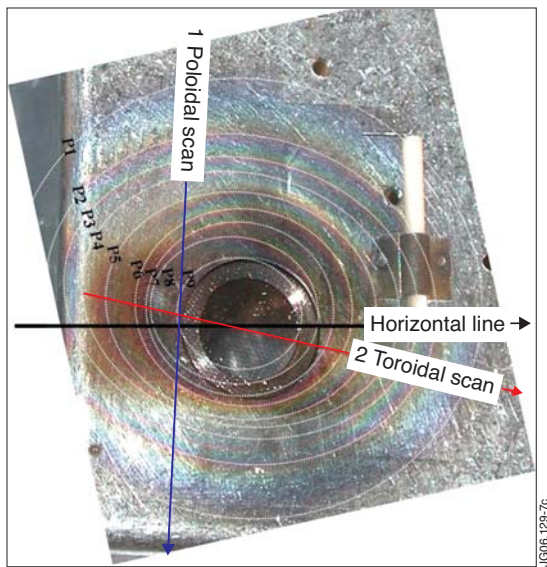

Figure 7: Colourful appearance of deposition layer on inner heat shield
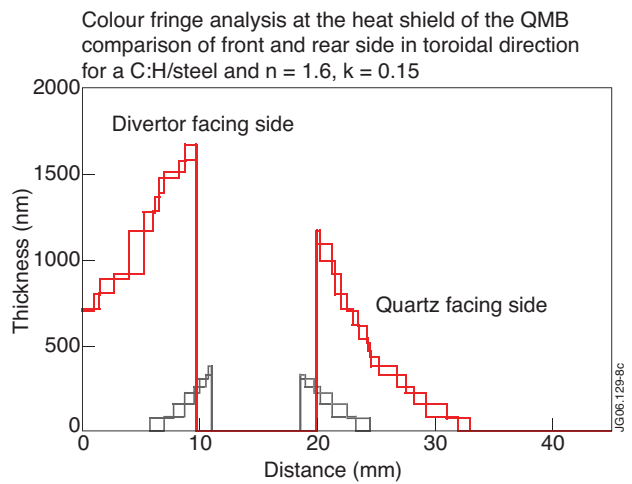

Figure 8: Line scans of areal carbon density on inner heat shield across orifice